

## Inclusive pion single-charge-exchange reactions

D. Ashery,\* D. F. Geesaman, R. J. Holt, H. E. Jackson, J. R. Specht, and K. E. Stephenson†  
Argonne National Laboratory, Argonne, Illinois 60439

R. E. Segel and P. Zupranski‡  
Northwestern University, Evanston, Illinois 60201

H. W. Baer, J. D. Bowman, M. D. Cooper, and M. Leitch  
Los Alamos National Laboratory, Los Alamos, New Mexico 87545

A. Erel  
Department of Physics and Astronomy, Tel Aviv University, Tel Aviv, Israel

J. Comuzzi and R. P. Redwine  
Physics Department, Massachusetts Institute of Technology, Cambridge, Massachusetts 02139

D. R. Tieger§  
Physics Department, Boston University, Boston, Massachusetts 02215  
(Received 15 February 1984)

The ( $\pi^+$ ,  $\pi^0$ ) and ( $\pi^-$ ,  $\pi^0$ ) reactions were studied on a variety of nuclei at a bombarding energy of 160 MeV. The full  $\pi^0$  energy spectra were measured with a  $\pi^0$  spectrometer at several detection angles. The energy spectra and angular distributions are characteristic of quasifree reactions. Effects due to multiple scattering, neutron screening, and Pauli blocking are clearly observed.

### I. INTRODUCTION

Studies of inclusive pion nucleus reactions make a significant contribution to the understanding of the propagation and interaction of  $\Delta$  resonances in the nuclear medium. Charged pion inclusive scattering has been studied quite extensively.<sup>1-3</sup> Both energy spectra and angular distributions are available over the whole periodic table and at several bombarding energies in the (3,3) resonance region. Recently, the inclusive double-charge-exchange (DCX) reaction was studied on a number of nuclei at several bombarding energies,<sup>4-6</sup> and yielded energy spectra and angular distributions. Previous information on inclusive single charge exchange (SCX) reactions is very limited—only one experiment provides energy spectra and angular distributions,<sup>7</sup> and a few others give total cross sections.<sup>8-10</sup> All these studies were performed at energies below the (3,3) resonance. The present work provides energy spectra and angular distributions for both ( $\pi^+$ ,  $\pi^0$ ) and ( $\pi^-$ ,  $\pi^0$ ) reactions for a variety of nuclei at 160 MeV. A preliminary account of the isospin effects observed in these data was published earlier.<sup>11</sup>

As in charged pion scattering, the SCX reaction is expected to proceed mainly through quasifree scattering, i.e.,  $\Delta$  formation and undisturbed decay. However, several effects arising from  $\Delta$ -nucleon interactions are expected to enhance<sup>12</sup> the multistep contributions to this reaction. Therefore, between the one-step-dominated charge pion scattering and the multi-step DCX reaction, there is the SCX reaction with comparable contributions from the two mechanisms. Analysis of this reaction should provide

information on the  $\Delta$ -nucleon interaction and the competition between  $\Delta$  absorption and decay in the nucleus.

### II. EXPERIMENTAL SYSTEM

In this work we present results of studies of the ( $\pi^+$ ,  $\pi^0$ ) and ( $\pi^-$ ,  $\pi^0$ ) reactions on the target nuclei listed in Table I. The experiment was performed in the low-energy pion channel at the Clinton P. Anderson Meson Physics Facility (LAMPF). The targets were bombarded with positive and negative 160-MeV pion beams whose flux was monitored by detecting muons from the pion decay. Two muon telescopes, each consisting of two NE-110 plastic scintillators, were mounted on the two sides of the beam so that both intensity and position stability of the beam could be monitored. These relative monitors were calibrated against the  $^{12}\text{C}(\pi, \pi\text{N})$  reaction cross section which

TABLE I. The nuclei studied in the ( $\pi^+$ ,  $\pi^0$ ) and ( $\pi^-$ ,  $\pi^0$ ) reactions, the target thicknesses, and isotopic enrichments.

( $\pi^+$ , $\pi^0$ )	( $\pi^-$ , $\pi^0$ )	Thickness (g/cm <sup>2</sup> )	Enrichment (%)
C	C	0.78	Natural
<sup>14</sup> C	<sup>14</sup> C	0.41	80
H <sub>2</sub> O	H <sub>2</sub> O	1.0	Natural
<sup>18</sup> H <sub>2</sub> O	<sup>18</sup> H <sub>2</sub> O	1.09	94.3
Ni		1.207	Natural
	<sup>120</sup> Sn	0.573	98.6
Pb	Pb	2.585	Natural

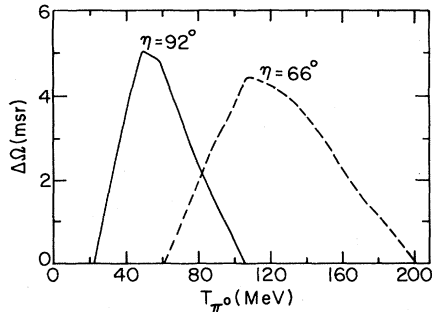


FIG. 1. Calculated acceptance curves for the  $\pi^0$  spectrometer positioned at  $108^\circ$ , for opening angles of  $92^\circ$  and  $66^\circ$  and distances to target of 52.5 cm and 80 cm, respectively. The actual acceptance is the calculated value multiplied by the conversion efficiency ( $\sim 0.34$ ; see Fig. 2).

was measured by activation analysis.<sup>13</sup> The calibration was repeated periodically and, in particular, each time the beam polarity was reversed. The results showed stability of better than 5%.

The outgoing neutral pions were detected in the horizontal plane using the LAMPF- $\pi^0$  spectrometer,<sup>14</sup> which measures the  $\pi^0$  energy by accurately measuring the opening angle between the two photons (from  $\pi^0$  decay) in wire chambers following converters and the total photon energy in total absorption Čerenkov counters. The spectrometer was operated in the "one post" mode, with the two arms mounted in the vertical plane. Two settings of the spectrometer were used: distances of 80 cm and 52.5 cm from the target and opening angles of  $66^\circ$  and  $92^\circ$ , respectively, for the high and low energy parts of the  $\pi^0$  spectrum, respectively. The acceptance of the spectrometer was calibrated by detecting the monoenergetic  $\pi^0$  mesons from the  $p(\pi^-, \pi^0)n$  reaction (using  $\text{CH}_2$  and carbon targets) for 27  $\pi^0$  energies between 32 and 163 MeV. This was achieved by using several bombarding energies (60, 75, 110, 130, and 160 MeV) and several scattering angles and by comparing the results with cross sections calculated from phase shifts.<sup>15</sup> The results were fitted to Monte Carlo calculations of the acceptance for the purpose of interpolation and matching of the two spectrometer settings. In Fig. 1 typical calculated acceptance curves are shown for the two settings. In Fig. 2 the ratio of measured to calculated acceptance is given as a function of  $\pi^0$  energy. This ratio is the conversion efficiency of the spectrometer

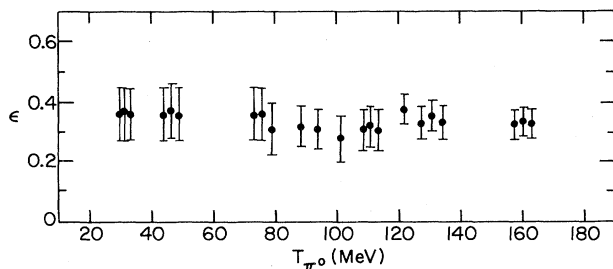


FIG. 2. The  $\pi^0$  spectrometer conversion efficiency ( $\epsilon$ ) obtained as a ratio of the measured and calculated acceptances.

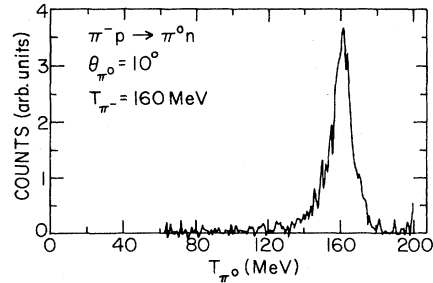


FIG. 3.  $\pi^0$  energy spectrum from the  $\pi^-p \rightarrow \pi^0n$  reaction, taken at  $10^\circ$  with the spectrometer at  $66^\circ$  opening angle.

(which is not included in the calculations), and its nearly constant value confirms the adequacy of the Monte Carlo calculations. The experimental conditions and the analysis were set for maximizing the counting rate while accepting modest energy resolution ( $\sim 10\%$  FWHM), which was sufficient for the inclusive nature of this study. A typical spectrum from the  $\pi^-p \rightarrow \pi^0n$  reaction obtained under these conditions is shown in Fig. 3. Since the spectrometer could cover approximately  $30^\circ$  in one position, the data were divided by software cuts into three angular bins of about  $10^\circ$  each. The spectrometer was positioned at central angles of  $10^\circ$ ,  $40^\circ$ ,  $70^\circ$ ,  $108^\circ$ , and  $153^\circ$ . Complete angular distributions were taken only for  $^{16}\text{O}$  and  $^{58}\text{Ni}$ ; for the other targets some angles are missing.

### III. RESULTS

Energy spectra from the  $(\pi^\pm, \pi^0)$  reactions detected at  $108^\circ$  are shown in Fig. 4. These spectra are obtained by matching at 85 MeV the data taken at the two spectrometer settings. As a consequence, discontinuities in the size of error bars are observed at this point in many spectra resulting from the different statistics taken at each setting. In the  $^{12}\text{C}(\pi^+, \pi^0)$  spectrum, a discontinuity appears also in the shape of the spectrum which could not be related to any normalization effect in a subsequent reexamination of the data. Since this is a steeply rising part of the spectrum, a small fluctuation in the lowest point of the high-energy part of the spectrum could account for most of this apparent discontinuity. All the spectra show a broad peak originating from a quasifree charge exchange mechanism. The energy spectra at all angles were integrated and a correction for the undetected fraction of the spectrum ( $E_{\pi^0} < 30$  MeV) was added. This correction ranges from a maximum of 15% for  $\text{Pb}(\pi^+, \pi^0)$  at backward angles to  $\lesssim 3\%$  at forward angles. The angular distributions deduced from these integrations are shown in Fig. 5. The errors include uncertainties in the low energy correction, angle-dependent acceptance uncertainty, and statistical errors. The uncertainty in the overall normalization is 10%. The lines in Fig. 5 represent the angular distribution for the  $p(\pi^-, \pi^0)n$  reaction, normalized to the data at backward angles. The normalization factors, denoted by  $N_{\text{eff}}$ , are listed in Table II. Also listed in this table are the angle-integrated cross sections, with the errors reflecting all contributions including angular integration and systematic normalization uncertainties.

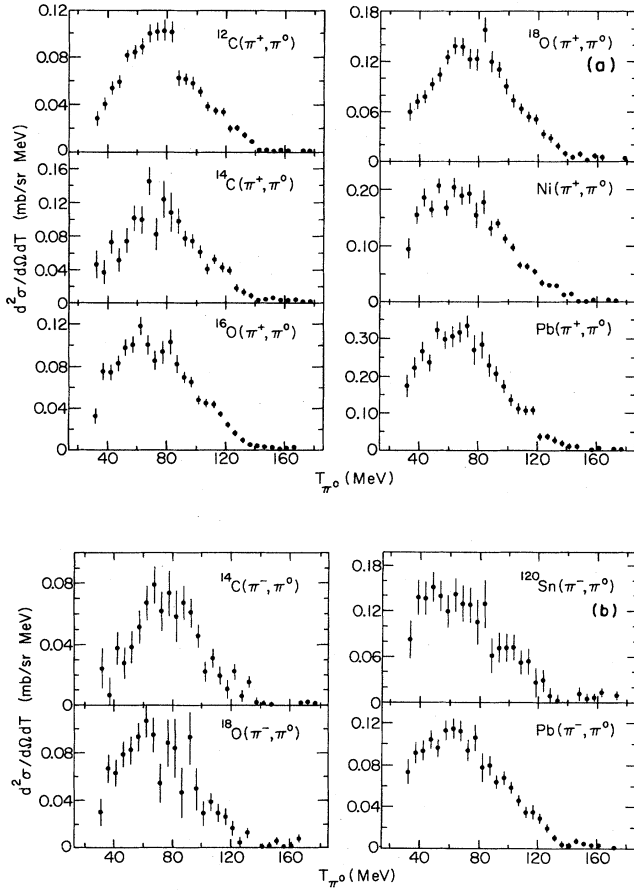


FIG. 4. (a)  $\pi^0$  energy spectra from the  $(\pi^+, \pi^0)$  reaction on the nuclei studied in the present work, taken at  $108^\circ$ . (b) Same as (a) for the  $(\pi^-, \pi^0)$  reaction.

The present results can be used to determine the true absorption cross section from measurements of the sum of cross sections for pion absorption and SCX.<sup>2</sup> The cross section estimates for the SCX reaction, made in Ref. 2, agree, within quoted uncertainties, with the results of the present work. While the precision of the present result is significantly better, due to the relatively small contribution of the SCX reactions, the absorption cross sections

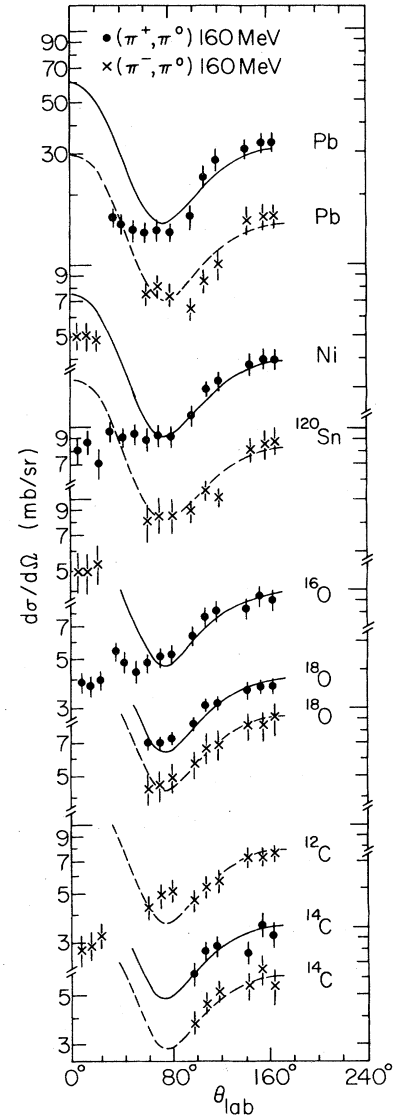


FIG. 5. Angular distributions from the  $(\pi^\pm, \pi^0)$  reactions.

TABLE II. The cross sections for  $(\pi^\pm, \pi^0)$  reactions at 160 MeV and the normalization factors of the  $\pi^-p \rightarrow \pi^0n$  reaction to the data for  $\theta \geq 90^\circ$ .  $B$  is the blocking ratio (see the text).  $N_{eff}$  is the factor which normalizes the cross section for  $p(\pi^-, \pi^0)n$  to the data observed at back angles for each nucleus.

	Nucleus	$\sigma_{cx}$ (mb)	$N_{eff}$	$B$
$\pi^\pm$	$^{12}\text{C}$	$64 \pm 10$	1.6	0.85
$\pi^+$	$^{14}\text{C}$		2.7	
$\pi^-$	$^{14}\text{C}$		1.3	
$\pi^\pm$	$^{16}\text{O}$	$80 \pm 12$	2.0	0.85
$\pi^+$	$^{18}\text{O}$	$110 \pm 16$	2.8	0.84
$\pi^-$	$^{18}\text{O}$	$73 \pm 15$	1.9	0.82
$\pi^+$	Ni	$158 \pm 20$	4.0	0.84
$\pi^-$	$^{120}\text{Sn}$	$127 \pm 25$	3.5	0.77
$\pi^+$	Pb	$252 \pm 30$	6.6	0.81
$\pi^-$	Pb	$113 \pm 16$	3.1	0.77

and error bars deduced in Ref. 2 are only slightly modified.

#### IV. DISCUSSION

In Fig. 6 the cross sections and  $N_{\text{eff}}$  values are plotted against  $Z$  for  $(\pi^-, \pi^0)$  and  $A - Z$  for  $(\pi^+, \pi^0)$ . In contrast with charged-pion scattering, where the cross sections and  $N_{\text{eff}}$  values increase monotonically<sup>2</sup> for both  $\pi^+$  and  $\pi^-$ , we note here a clear difference. The cross sections and  $N_{\text{eff}}$  values for the  $(\pi^+, \pi^0)$  reaction behave very similarly to charged pion scattering: The cross section increases as  $(A - Z)^{0.45}$  (or as  $A^{0.48}$ ) and  $N_{\text{eff}}$  as  $(A - Z)^{0.46}$  (the corresponding power for charged pion scattering<sup>2</sup> is 0.43). On the other hand, both cross section and  $N_{\text{eff}}$  values for the  $(\pi^-, \pi^0)$  reach saturation for  $A \sim 100$ . A similar and enhanced effect is observed for the DCX reaction,<sup>5,16</sup> where  $\sigma(\pi^+, \pi^-) \sim A^{0.8}$ , while  $\sigma(\pi^-, \pi^+)$  saturates for  $A > 40$ . The reason for this effect may come from two sources. In neutron-rich nuclei the protons, which are the interacting nucleons for the quasifree  $(\pi^-, \pi^0)$  reaction, are screened by the excess neutrons. This screening is very effective since negative pions interact strongly with neutrons. An additional source can be stronger Pauli blocking for the  $(\pi^-, \pi^0)$  reaction on heavy nuclei since there are several occupied neutron shells above the valence proton shell where most of the quasifree reaction can occur. Pauli blocking effects are particularly noticeable at forward angles, where the momentum transferred to the recoiling nucleon is relatively small. In fact, the angular distributions look different for  $(\pi^+, \pi^0)$  and  $(\pi^-, \pi^0)$  at forward angles, with a somewhat stronger suppression for the latter reaction.

The effect of the Pauli blocking can be estimated by the difference between the measured cross section and that for the free process. In Table II we list the ratio

$$B = \sigma_{\text{cx}} / [N_{\text{eff}} \times \sigma(\pi^- p \rightarrow \pi^0 n)].$$

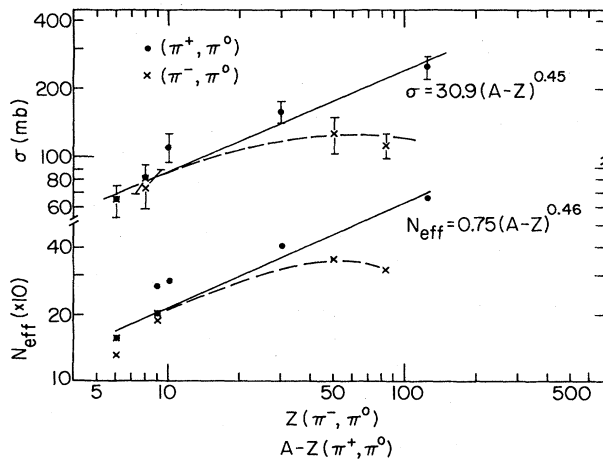


FIG. 6. Cross sections and  $N_{\text{eff}}$  values plotted against  $Z$  for  $(\pi^-, \pi^0)$  reactions and against  $(A - Z)$  for  $(\pi^+, \pi^0)$  reactions.  $N_{\text{eff}}$  is the factor which normalizes the cross section for  $p(\pi^-, \pi^0)n$  to the data observed at back angles for each target.

The cross section for the  $\pi^- p \rightarrow \pi^0 n$  reaction is taken as<sup>17</sup>  $47 \pm 0.5$  mb. The value of  $B$  is seen to be nearly constant, about 0.83, similar to the value observed for charged pion scattering.<sup>2</sup> The two smaller values are for Pb and Sn  $(\pi^-, \pi^0)$ , suggesting stronger blocking.

It is instructive to compare the yields from  $(\pi^-, \pi^0)$  reactions on Pb and C. At backward angles [Fig. 7(a)] both spectra show a quasifree reaction peak and the ratio (2.4) is very similar to that found<sup>1</sup> for  $(\pi^+, \pi^+)$  scattering on these two nuclei (2.5, but  $\sim 10\%$  of the cross section is scattering from neutrons). This may indicate that at these angles neutron screening effects are not strong. At smaller angles the ratio for  $(\pi^-, \pi^0)$  decreases gradually to  $\sim 1.6$  at  $90^\circ$  [for  $(\pi^+, \pi^+)$  it is steady over this angular range]. From this angle on to forward angles the ratio does not change, but, as can be seen in Fig. 7(b), the two spectra look quite different at forward angles. In the quasifree peak the cross section ratio is 1 and the total ratio becomes 1.7 for the large multiple scattering tail in Pb. The quasifree  $(\pi^-, \pi^0)$  reaction cross section being equal for C and Pb at forward angles is yet another manifestation of the strong blocking (or enhanced screening compared with backward angles) for this reaction. The  $(\pi^+, \pi^0)$  reaction also shows a behavior which is similar to charged pion scattering: a fixed ratio ( $\sim 4.5$ ) at back angles which decreases in the region of the minimum in the angular distribution. The energy spectra for  $(\pi^+, \pi^0)$  and  $(\pi^+, \pi^+)$

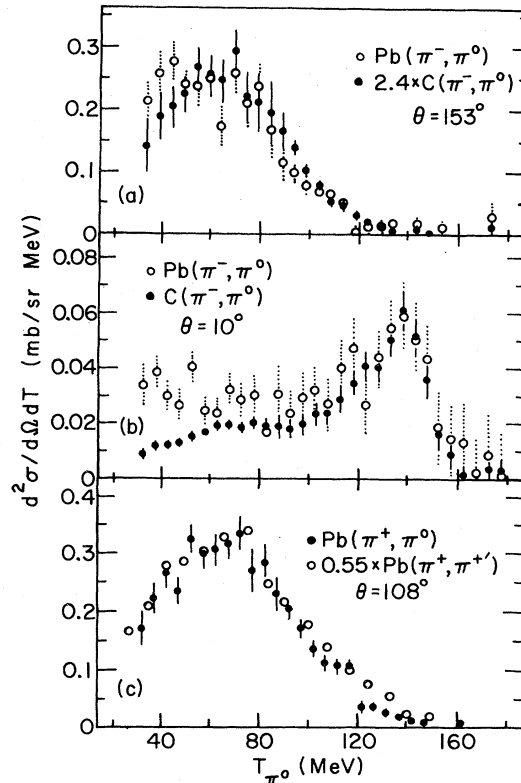


FIG. 7.  $\pi^0$  energy from the C  $(\pi^-, \pi^0)$  and Pb  $(\pi^-, \pi^0)$ . (a) Spectra are at  $153^\circ$  and the C spectrum is multiplied by 2.4. (b) Spectra at  $10^\circ$ . (c) Spectra at  $108^\circ$  from Pb  $(\pi^+, \pi^0)$  and Pb  $(\pi^+, \pi^+)$ , the latter spectrum (Ref. 1) multiplied by 0.55 and shifted by a  $Q$  value of 10 MeV.

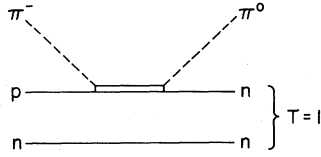


FIG. 8. The  $(\pi^-, \pi^0)$  reaction as an isovector transition.

are compared in Fig. 7(c).

The process of multiple scattering brings another input to the question of  $\Delta$  dynamics in the nuclear medium. When formed, the  $\Delta$  faces competition between decay, absorption ( $\Delta N \rightarrow NN$ ), and  $\Delta N$  scattering. For the first and second transitions we have elementary processes for comparison: The free  $\Delta$  decay is known, and in the nucleus it will be quenched by the factor  $B$  ( $\sim 0.8$ ) discussed above. The  $\Delta N \rightarrow NN$  transition is known from studies of pion absorption on  $T=0$  nucleon pairs in the deuteron. Multiple scattering gives us a way to compare the  $\Delta N$  scattering with the two other processes. In the case of the SCX reaction, several factors enhance these multistep processes.<sup>12,16</sup> First, there is the relative weakness of the one-step process (compared with charged pion scattering) which allows multistep effects to be more easily observed. The second is the  $\Delta T=1$  nature of the SCX reaction. For charged pion scattering, multistep processes are truncated by pion absorption: the  $\Delta N \rightarrow NN$  process. This transition is strong due to the formation of the intermediate  $\Delta N$  system in a  ${}^3S_2$   $T=1$  state, where the  $\Delta$  and the nucleon are in a relative  $s$  state. In the SCX reaction, if the  $\Delta$  interacts with a nucleon, the  $\Delta N$  system cannot have the  ${}^5S_2$   $T=1$  quantum numbers since such a state cannot couple to the final two-nucleon state (see Fig. 8). This final state will be a nucleon pair with  $T=1$  in a relative  ${}^1S_0$  state for low momentum transfer. Simple parity, angular momentum, and isospin selection rules forbid this coupling. Consequently, it may be expected that multistep processes in the SCX reaction will not be as strongly truncated as in charged pion scattering. This is also referred to as cancellation of the medium correction for isovector excitations.<sup>12,16</sup>

These effects can be observed by comparing the results of the present work to charged pion scattering and to the DCX reactions. In Fig. 9 we show the low energy part of the outgoing pion spectrum at  $30^\circ$  in the  $(\pi^+, \pi^+)$  (Ref. 3),  $(\pi^+, \pi^0)$ , and  $(\pi^+, \pi^-)$  (Ref. 5) reactions on  ${}^{16}\text{O}$  at 160 MeV. This part of the spectrum is particularly sensitive to multiple scattering. The spectra are scaled by the undistorted predictions of the two-step process (based on the Clebsch-Gordan coefficients):  $\pi^+ : \pi^0 : \pi^- = 26:9:1$ . The  $\pi^0$  and  $\pi^-$  spectra are also shifted by the appropriate

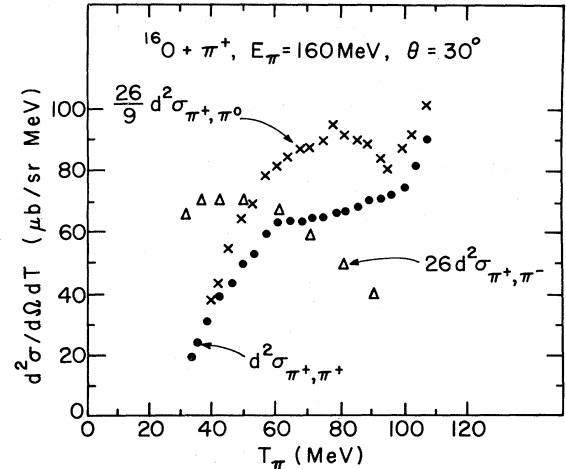


FIG. 9. Low energy part of the  $\pi^+$  spectrum from the  ${}^{16}\text{O}(\pi^+, \pi^+)$  reaction (Ref. 3), of the  $\pi^0$  spectrum from the  ${}^{16}\text{O}(\pi^+, \pi^0)$  reaction multiplied by  $\frac{26}{9}$ , and the  $\pi^-$  spectrum from the  ${}^{16}\text{O}(\pi^+, \pi^-)$  reaction (Ref. 5) multiplied by 26. The  $\pi^0$  and  $\pi^-$  spectra also are shifted by the appropriate  $Q$  value. All spectra are for  $E(\pi^+) = 160$  MeV, where the  $\pi^-$  spectrum is interpolated between the 150 and 180 MeV data.

$Q$  value. As can be seen, the SCX (relative) yield is significantly higher than for the other two (normalized) reactions. This is consistent with predictions by Hirata *et al.*<sup>18</sup> that for  $(\pi^+, \pi^0)$  reactions the ratio of the second to first order term is  $\sim 30\%$  larger than for  $(\pi^+, \pi^+)$  reactions.

In conclusion, we have presented results of systematic studies of the  $(\pi^\pm, \pi^0)$  reactions at 160 MeV. In contrast to charged pion scattering, the combination of neutron screening and Pauli blocking effects causes a significantly different  $A$  dependence of the cross section between  $\pi^+$  and  $\pi^-$ . The effects of the multistep reaction mechanism are strong and may be used to understand the  $\Delta N$  rescattering contribution to the medium corrections affecting  $\Delta$  propagation in nuclei.

#### ACKNOWLEDGMENTS

The authors would like to thank the LAMPF operating staff for their support in the course of this experiment. One of us (D.A.) would like to acknowledge the warm hospitality of Argonne National Laboratory. This research was supported in part by the U.S. Department of Energy and the National Science Foundation.

\*Permanent address: Tel Aviv University, Tel Aviv, Israel.

†Present address: EMR Photoelectric, Box 44, Princeton, NJ 08540.

‡Permanent address: Institute for Nuclear Research, Warsaw, Poland.

§Present address: University of Washington, Seattle, WA 98195.

<sup>1</sup>S. M. Levenson *et al.*, Phys. Rev. C 28, 326 (1983).

<sup>2</sup>D. Ashery *et al.*, Phys. Rev. C 23, 2173 (1981).

<sup>3</sup>C. H. Q. Ingram *et al.*, Phys. Rev. C 27, 1578 (1983).

- <sup>4</sup>R. E. Mischke *et al.*, Phys. Rev. Lett. **44**, 1197 (1980).  
<sup>5</sup>S. A. Wood, Ph.D. thesis, MIT, 1983 (unpublished).  
<sup>6</sup>J. Davis *et al.*, Phys. Rev. C **20**, 1946 (1979).  
<sup>7</sup>T. J. Bowles *et al.*, Phys. Rev. C **23**, 439 (1981).  
<sup>8</sup>E. Bellotti, S. Bonetti, D. Cavalli, and C. Matteuzzi, Nuovo Cimento **14A**, 567 (1973).  
<sup>9</sup>H. Hilscher, W. D. Krebs, G. Sepp, and V. Soergel, Nucl. Phys. **A158**, 602 (1970).  
<sup>10</sup>J. Alster and J. Warczawsky, Phys. Rep. **52**, 87 (1979).  
<sup>11</sup>D. Ashery *et al.*, Phys. Rev. Lett. **50**, 482 (1983).  
<sup>12</sup>M. Thies, in Proceedings of the Symposium on Delta-Nucleus Dynamics, Argonne, 1983, p. 115.  
<sup>13</sup>B. J. Dropesky *et al.*, Phys. Rev. C **20**, 1844 (1979).  
<sup>14</sup>H. W. Baer *et al.*, Nucl. Instrum. Methods **180**, 445 (1981); S. Gilad, Ph.D. thesis, Tel Aviv University, 1979 (unpublished).  
<sup>15</sup>G. Rowe, M. Salomon, and R. H. Landau, Phys. Rev. C **18**, 584 (1978).  
<sup>16</sup>C. H. Q. Ingram, in Proceedings of the Symposium on Delta-Nucleus Dynamics, Argonne, 1983, p. 55.  
<sup>17</sup>D. V. Bugg *et al.*, Nucl. Phys. **B26**, 588 (1971).  
<sup>18</sup>M. Hirata, F. Lenz, and M. Thies, Phys. Rev. C **28**, 785 (1983).